

Article

Thermal-Energy Analysis and Life Cycle GHG Emissions Assessments of Innovative Earth-Based Bamboo Plastering Mortars

Rayane de Lima Moura Paiva ¹, Lucas Rosse Caldas ^{1,2}, Adriana Paiva de Souza Martins ¹,
Patricia Brandão de Sousa ², Giulia Fea de Oliveira ² and Romildo Dias Toledo Filho ^{1,*}

¹ Programa de Engenharia Civil (PEC), COPPE, Federal University of Rio de Janeiro, Rio de Janeiro 21941-972, Brazil; rayane@coc.ufrj.br (R.d.L.M.P.); lucas.caldas@fau.ufrj.br (L.R.C.); adriana@numats.coc.ufrj.br (A.P.d.S.M.)

² Programa de Pós-Graduação em Arquitetura (PROARQ), Faculty of Architecture and Urbanism, Federal University of Rio de Janeiro, Rio de Janeiro 21941-901, Brazil; patricia.sousa@fau.ufrj.br (P.B.d.S.); giulia.oliveira@fau.ufrj.br (G.F.d.O.)

* Correspondence: toledo@coc.ufrj.br

Abstract: Biomaterials and raw earth have demonstrated a promising potential for improving various thermal properties of plastering mortars used in buildings. The objective of this research was the evaluation of the thermal-energy performances and life cycle greenhouse gas (GHG) emissions of different mixtures of engineered, bio-based earth mortars composed of bamboo particles, earth, and different cementitious materials. Four mixtures were assessed: mortars without bamboo particles (matrix), and mortars containing 3%, 6%, or 9% of bamboo particles by volume. The bulk density and thermal conductivity values obtained for the matrix and mortars with the highest percentage of bamboo particles (9%) were 1704.13 and 1471.80 kg/m³, and 0.62 and 0.43 W/M·K, respectively. Based on experimental results, thermal-energy simulations were carried out using a social housing project as a case study. The simulations evaluated different climate conditions and applied life cycle GHG emissions assessment methodology. Compared with typical cement and lime plastering mortars, the proposed bio-based earth mortars presented a superior thermal-energy performance and lower GHG emissions, particularly the 9% bamboo particles mixture. GHG emissions reached a maximum decrease of 28%. The main scientific contribution of this research is the presentation of an engineered, bio-based earth mortar that can be manufactured using local raw materials available in most developing countries with significant housing demands. The method used, based on experimental research, thermal-energy analysis, and life cycle GHG emissions, may be used for evaluating other innovative materials. It was verified that even with thin plastering in buildings, it is possible to achieve energy efficiency gains and to reduce GHG emissions.

Keywords: plasters; raw earth; plant-based materials; thermal-energy performance; carbon footprint; LCA



Citation: Paiva, R.d.L.M.; Caldas, L.R.; Martins, A.P.d.S.; de Sousa, P.B.; de Oliveira, G.F.; Toledo Filho, R.D. Thermal-Energy Analysis and Life Cycle GHG Emissions Assessments of Innovative Earth-Based Bamboo Plastering Mortars. *Sustainability* **2021**, *13*, 10429. <https://doi.org/10.3390/su131810429>

Academic Editors: Antonio Caggiano and Jorge S. Dolado

Received: 12 August 2021

Accepted: 6 September 2021

Published: 18 September 2021

Publisher's Note: MDPI stays neutral with regard to jurisdictional claims in published maps and institutional affiliations.



Copyright: © 2021 by the authors. Licensee MDPI, Basel, Switzerland. This article is an open access article distributed under the terms and conditions of the Creative Commons Attribution (CC BY) license (<https://creativecommons.org/licenses/by/4.0/>).

1. Introduction

Buildings and the construction sector are together responsible for 35% of global energy consumption and 38% of total emissions [1]. In the European Union, the built environment accounts for 40% of total energy demand and 36% of carbon emissions [2]. The Intergovernmental Panel on Climate Change [3] has predicted that, by the middle of this century, the energy use of the building sector will almost double, and carbon dioxide (CO₂) emissions will increase by 50% to 150%. In this context, more efficient building design will play a crucial role in reducing the negative impacts associated with energy consumption and the emission of pollutants. In general, the best strategy for the design of zero or near-zero energy buildings and the retrofitting of existing buildings is: firstly,

reducing energy demands by considering efficiency measures, especially those acting on the envelope and equipment; and secondly, introducing renewable energy systems [4,5]. Regarding the envelope, the incorporation of insulating materials has shown to be an efficient practice for reducing operational energy use, principally in temperate and cold climates [6–9].

Raw earth-based materials can be used in envelopes to improve thermal and energy performance [10–12]. The use of these materials as building components has many sustainability credentials: it is natural, commonly locally available, abundant, non-toxic, low in embodied energy and carbon, has good thermal properties, and is recyclable [5,6].

Earth mortars have received increasing attention from the scientific community for their ability to positively influence the heat and moisture fluxes that occur in building envelopes, thereby providing indoor environments with greater environmental comfort and health, as well as reducing the need for artificial air conditioning [13–17].

Other important alternatives are bio-based materials, which have been used as building materials since the beginning of civilization [18]. The necessary biomass can be obtained from planted forests (pine or eucalyptus, among others), agricultural resources (rice sugar cane, wheat, corn, oat, barley, rye, among others), various plants (sisal, jute, curauá, coconut, hemp, flax, rush, miscanthus, sunflower, among others), bamboo, and residues from raw vegetable material processing [19–21]. Plant particles can be used in the form of aggregates, fibers, or ash in raw earth or cementitious matrices, and are characterized by high multiscale porosity, low density and high hygroscopicity, resulting in composites that are functionally optimized for thermal insulation and thermohygric regulation applications [22]. When the biomass incorporated into the matrix comprises residues from the processing of primary plant resources, factors such as the renewability of the raw material, the ability to sequester CO₂, and the valorization of the residue can effectively contribute to the matrix's suitability for low-carbon and energy solutions [23–28]. In addition to the plant resources already mentioned, algae can be successfully used as a resource of bio-based materials for the production of insulating coating materials. Caniato et al. [29] and Caniato et al. [30] produced open-cell foams based on alginate (polymer extracted from the cell walls of brown algae) for thermal and sound insulation applications. Those composites showed good insulation properties and did not require energy-intensive processes for production, unlike those commonly used in the production of commercial foams.

In the literature, there are many reports of plastering mortars based on earth and vegetable particles. However, most of these studies incorporated biomasses from temperate species, such as wheat and barley straw [10,15], hemp [12,14], and olive tree pruning [17] waste. The thermal properties of 13 plant biomass were reviewed by Asdrubali et al. [19]. The authors highlighted the observation that biomass products can be advantageous for thermal insulation applications, compared with conventional insulators (polystyrene, rock wool and glass wool), as they are based on renewable resources and do not require energy-intensive production processes. Binici et al. [31] used plant biomass waste in the production of insulating composites (mortars and panels). The thermal properties complied with current regulations, creating a more environmentally appropriate route for waste recycling than the current practices of burning waste, which are associated with high CO₂ emissions.

The influences of the incorporation of plant particles in earth matrices were reviewed by Laborel-Préneron et al. [18]. For a given volumetric fraction of plant particles, the resulting matrices exhibited vastly different values of bulk density and thermal conductivity, depending on the type of plant (raw material source), the other constituents and the composite production process. Coconut fibers incorporated into conventional mortars reduced energy consumption and increased thermal comfort in a low-income area that is subject to a tropical climate, improving the habitability of the homes and the well-being of the inhabitants [32].

Amziane and Sonebi [21] reviewed the multiple possibilities for developing building materials based on bio aggregates and mineral binders. The high porosity and low bulk

density of bio aggregates provide the composites with good thermal properties, resulting in more efficient buildings in terms of energy and CO₂ emissions, improving both air quality and the occupants' health. The insulating behavior of earth mortars was improved when the vegetable fiber content varied from 4% to 12% (in relation to the total mass of the composite), with a reduction in bulk density and an increase in porosity [17]. Although there are several papers in the literature on the use of bamboo as a structural element in concrete and other construction applications [33–36], there is a scarcity of data about bamboo particles used in earth-based plastering mortars.

It is estimated that by 2050 half of the world's population will reside in urban, tropical regions, located mainly in the African, Asian, and Latin American continents [25], demanding an increased thermal comfort in these regions, where bamboo can be found as an easily available bio-based resource. Bamboo is a rapidly renewable resource and in its growing phase captures atmospheric CO₂ and stores it in its tissues. When bamboo is used in a durable building material production, the sequestered carbon remains stored throughout the building's life. Plantations are perennial, capturing CO₂ and readily producing raw material for its potential use as a building material [37].

One way that is frequently used to evaluate the potential environmental impacts of building products is the life cycle assessment (LCA) methodology, or life cycle greenhouse gas (GHG) emissions assessment, wherein only the global warming potential impact is evaluated [38–40]. Melià et al. [13] used the LCA to evaluate unstabilized earth mortars and verified a superior environmental performance compared with conventional mortars, with the largest impact component for both being the energy obtained from fossil sources. Santos et al. [41] reviewed existing literature that addresses the LCA of cementitious mortars, highlighting the existence of only few studies for earth mortars. By using LCA, Caldas et al. [42] verified that earth plasters could present gains of up to 80% for the global warming impact category when compared with conventional mortars. Both of these studies focus only on the production stage, maintenance, and end-of-life of mortars. None of them evaluated the benefits in terms of operational energy reduction that these earth mortars can bring when used in building façades. The present research also advances in this area.

There has been an impressive amount of research using LCA for building product studies in the last few years. However, there is little focus on tropical countries, especially South American countries, in the literature [43,44]. The present study can contribute significantly to overcoming this shortcoming. In addition, there is little research on earth-engineered mortars and even less when considering the use of bamboo particles. This research links experimental data with thermal-energy simulations and LCA, delivering a holistic approach to a novel and non-conventional material. This mortar can be produced where bamboo and cementitious materials are available, which is the case in many developing countries, being able to meet a substantial housing demand for new buildings in the coming years.

This study aims at performing a thermal-energy analysis and evaluating the life cycle GHG emissions (the carbon footprint) of different wall configurations employing engineered bio-based earth mortars developed in a laboratory and produced with bamboo particles (EMB). The EMB are composed of raw earth, cementitious materials (Portland cement, hydrated lime, metakaolin, and fly ash), chemical additives, and water. Mixtures with 0%, 3%, 6%, and 9% of bamboo particles (in volume) are appraised. A case study of a social housing project in Brazil has been carried out that considers three cities (Curitiba, Teresina, and Rio de Janeiro) located in tropical and temperate regions. For the thermal-energy analysis and the life cycle GHG emissions, the EMB are compared with conventional mortar systems (CMS) made of cement and hydrated lime. For the experimental evaluation in the laboratory of EMBs, the EMB9 is compared with EMB0 (without bamboo particles).

2. Materials and Methods

This research was carried out using experimental data collected in the laboratory and GHG emissions life cycle modeling (using the LCA methodology). For this, the methods were divided into (1) characterization of materials, (2) productions and characterization of

EMB and CMS, (3) life cycle GHG emissions assessment, and (4) thermal energy simulation. EMB0 was the experimental “control” mixture. For the thermo-energy simulation and the life cycle GHG emissions assessment the CMS was additionally used, and this system was declared “reference” to avoid misunderstanding.

2.1. Materials

The binding materials used in this research consisted of fine earth fractions ($E_{ff} = \emptyset < 0.06$ mm), hydrated lime (HL), Brazilian high initial strength Portland cement (CPV), metakaolin (MK), and fly ash (FA). Table 1 summarizes the true density and chemical composition of the binding materials obtained by the helium gas pycnometer method (Accupyc by Micromeritics) and X-ray fluorescence (FRX) in a Shimadzu EDX-720 spectrometer.

Table 1. Physical and chemical properties of binders.

| | Hydrated Lime (HL) | Portland Cement (CPV) | Metakaolin (MK) | Fly Ash (FA) | Earth (E) |
|-----------------------------------|--------------------|-----------------------|-----------------|--------------|-----------|
| True Density (kg/m ³) | 2530 | 3010 | 2690 | 1940 | 2680 |
| Oxide composition by mass (wt.%) | | | | | |
| CaO | 64.66 | 57.04 | 0.14 | 1.81 | 3.99 |
| SiO ₂ | 3.09 | 22.06 | 44.90 | 52.33 | 51.30 |
| Al ₂ O ₃ | - | 10.44 | 44.42 | 33.15 | 26.07 |
| Fe ₂ O ₃ | 0.33 | 1.73 | 4.88 | 4.82 | 10.76 |
| SO ₃ | 0.61 | 3.87 | 1.45 | 1.86 | 1.27 |
| K ₂ O | 0.30 | 0.54 | 1.42 | 3.46 | 4.41 |
| MgO | 30.97 | - | - | - | - |
| Sc ₂ O ₃ | - | 3.58 | - | - | - |
| TiO ₂ | - | - | 1.37 | 1.14 | 1.75 |
| P ₂ O ₅ | - | - | 0.93 | 0.76 | - |

Aggregates consisted of natural sand (NS) with a maximum diameter of 850 μ m and true density of 2650 kg/m³, coarse earth fractions ($E_{cf} = \emptyset > 0.06$ mm) with a true density of 2680 kg/m³ and bamboo particles (BP). Figure 1 shows the granulometric curves of the binding materials obtained by using a laser granulometer (Malvern Mastersizer[®] 2000) and of the E_{cf} and NS aggregates obtained from NBR 6457 [45] and NBR NM 248 [46], respectively.

According to Restrepo et al. [47] and Escamilla and Habert [37], the losses and consequent generation of waste from the use of bamboo in a more industrialized way, commonly applied in the construction sector, such as fabrics, sheets or glued laminates can reach around 40–60% by mass. Bamboo particles (BP) were produced from waste from the architecture sector in the state of Rio de Janeiro (Brazil). The bamboo species, *Bambusa chungii*, was used without any pre-treatment. First, the length of the bamboo waste was reduced to 30 cm with a Makita circular saw model MLT100 (Figure 2a). After cutting, the residue was processed in a Fragmaq brand, industrial, civil construction factory to obtain the first particles with a length between 4 and 10 cm (Figure 2b). Then with the aid of a Primotécnica model LP 1003 knife mill (Figure 2c), the particles were reduced and separated by passing them through square mesh sieves with a nominal opening of 600 μ m and 300 μ m with a length between 0.6 and 2 cm (Figure 2d). The bamboo particles used in the mortars’ production were resultant of the mixture of equal parts of those retained in the sieves of 300 μ m and 600 μ m. The bulk density, moisture content and water absorption were 500 kg/m³, 8.5%, and 61.7%, respectively, according to NM 52 [48] and NBR 9939 [49], and the methodology adopted was by Da Gloria et al. [34] with adaptations for the molding time ($t = 4$ min).

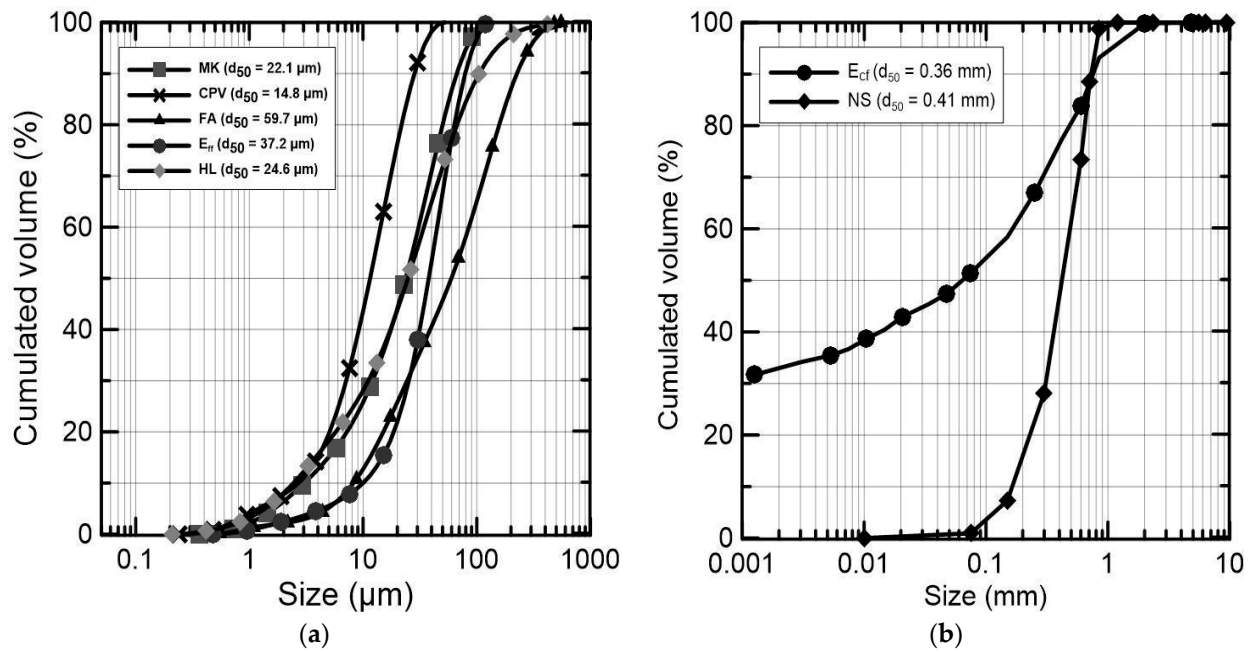


Figure 1. Particle size curves. (a) binding materials and (b) aggregates E_{fc} and NS.



Figure 2. Bamboo particles obtained during processing. (a) Bamboo pole waste, (b) First processing, (c) Second processing, and (d) bamboo particles used in this research.

The morphological characterization of the bamboo particles used was performed using an Aggregate Image Equipment Measurement System (AIMS), according to the standard AASHTO TP81 [50]. The AIMS is capable of providing up to five distinct properties for aggregates. Among them, three are applied to coarse aggregates (sphericity, surface texture, and flatness/elongation ratio), one to fine aggregates (shape 2D), and the last one (angularity index) can be applied to coarse and fine aggregates. For the present study, only two properties were considered: the angularity index, which describes the variations in the contour of the particles analyzed using a gradient method, ranging from 1 (perfect circle) to 10,000 and the shape 2D index that is directly related to the shape of a circle, providing three-dimensional measurements (width, length, and thickness) and varies from 0 (for circular particles) to 20. According to the classifications proposed by Masad [51], bamboo particles were classified as “sub-rounded” because the average angularity index obtained was 3828 and “elongated” for the 2D shape where the average value obtained was 15.24. In Figure 3, some images obtained during the test are presented.

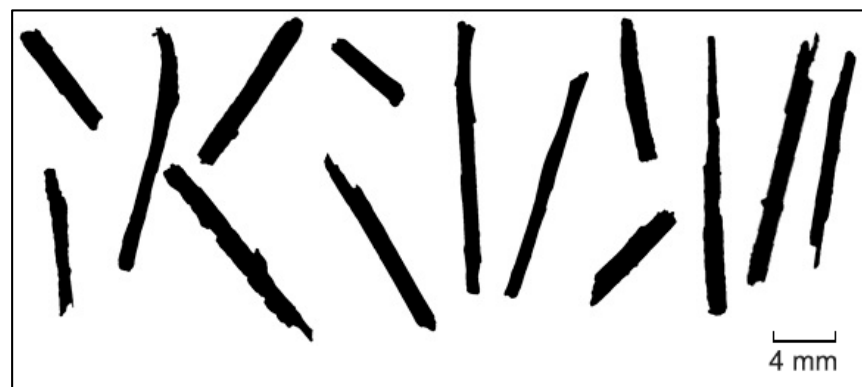


Figure 3. Morphology of bamboo particles.

Bamboo particles were characterized by microstructural analysis using a scanning electron microscope (SEM) TM 3000. In Figure 4, it is possible to observe that the morphology of bamboo particles presents a porous tubular structure formed by a mixture of parenchymal cells and several vascular bundles of fibrous structure, where most of the hollow cell cavities are filled with air, which justifies the literary value for the bulk density and high-water absorption potential of the particles.

The other constituents used in the production of mortars (EMB) were the superplasticizer Glenium 51 (SP), water (W) and calcium chloride (CaCl_2) as an accelerator for cement hydration. The superplasticizer was used in small quantities and normally replaces a high number of cementitious materials (due to the water reduction in the mixture and the fewer cementitious materials required). In the case of mortars, the superplasticizer commonly replaces cement and hydrated lime, as literature shows [52,53], without compromising the rheology. The cementitious materials, and especially lime, are the most GHG emission-intensive mortars constituents. The conventional mortar system (CMS) was selected to obtain results from an industrial mortar coating regularly used in the Brazilian construction sector.

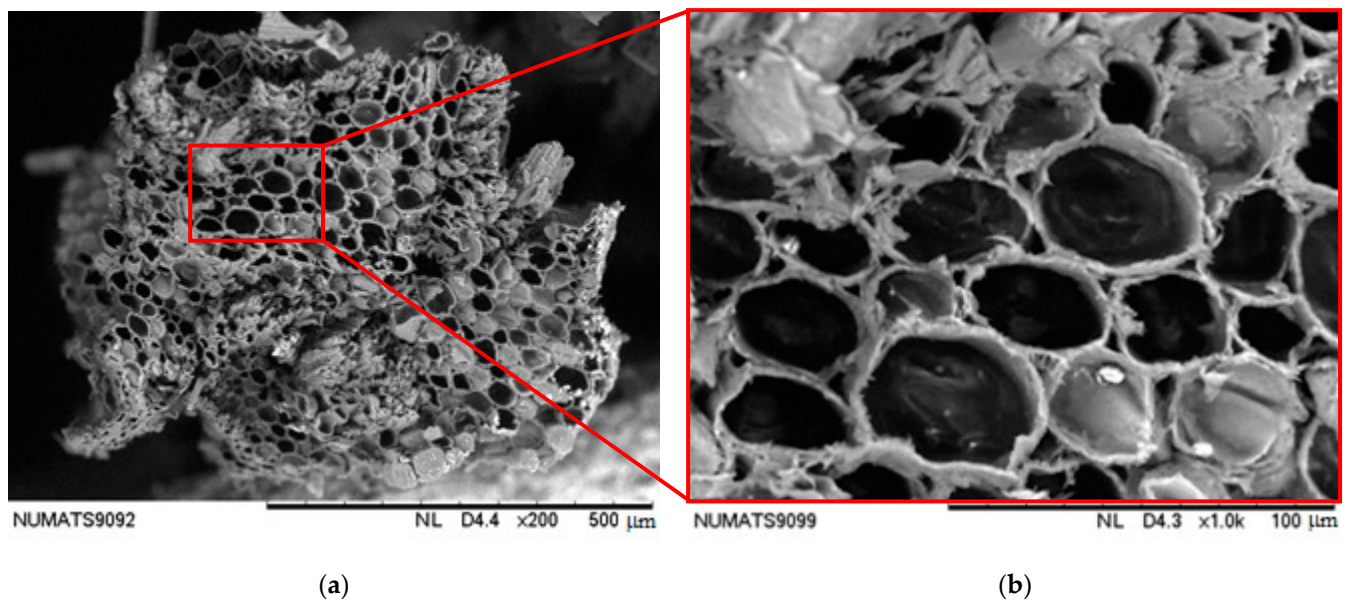


Figure 4. Bamboo particle SEM. (a) 200× cross-sectional area and (b) 1.0 k cross-sectional area.

2.2. Mixture Proportions and Production

For the earth mortar matrix (EMB0) production, the mass ratio used in the dosage was 1: 3 (binder material: aggregate). The dosage of this matrix occurred from the characteristic of the fine fraction of earth ($E_{ff} = \emptyset < 60 \mu\text{m}$), which is therefore the main constituent of the total binding materials (100%), corresponding to the consumption of 226.24 kg/m^3 (49%). In order to produce a low environmental impact mortar, a complete range of binders was used: 92.34 kg/m^3 of hydrated lime (20%), 50.79 kg/m^3 of fly ash (11%), 46.17 kg/m^3 of high early strength Portland cement (10%) and 46.17 kg/m^3 of metakaolin (10%).

The aggregates used consist of 235.47 kg/m^3 the coarse earth fraction ($E_{cf} = \emptyset > 60 \mu\text{m}$) (17%) and 1149.65 kg/m^3 natural sand ($\emptyset < 850 \mu\text{m}$) (83%). The water-binder material ratio (w/bm) used was determined from the preparation of previous mixtures until a minimum consistency of approximately $180 \pm 20 \text{ mm}$ was obtained and subsequently fixed at 0.65. The other constituents used were dosed in relation to the mass of the binder materials, consisting of 9.23 kg/m^3 of Glenium 51 superplasticizer (2%), and 4.62 kg/m^3 of calcium chloride (CaCl_2) (1%) which used as an accelerator of cement hydration, with the aim of decreasing the initial setting.

The production of earth mortar with percentages of 3%, 6%, and 9% of bamboo particles (EMB3, EMB6, and EMB9, respectively) was based on values from EMB0. The amount of binding material, the w/bm ratio, the CaCl_2 content were the same as used in EMB0. Due to the physical and morphological characteristics of the BP, it was necessary to reduce the natural sand content to guarantee the overall mixture volume (1 m^3).

However, the superplasticizer content had to be adjusted to 3% to ensure the minimum consistency determined. The total water of the mixture (W_t) was the sum of the BP compensating water (61.7%) and the hydration water calculated from the water-binder material ratio. The material consumption adjusted in kg/m^3 as a function of the insertion of bamboo particles is shown in Table 2.

The production of mortars started with dry mixing the binding materials with the aggregates. Once the materials were homogenized, half of the water was slowly introduced for 3 min, followed by the gradual addition of the superplasticizer for 5 min and calcium chloride for 1 min, both diluted in the rest of the water. After completing 9 min of mixing, the bamboo particles were inserted slowly to ensure a homogeneous dispersion (Figure 5a). The total mixing time was 14 min. The material was molded in single layers in square molds measuring $10 \times 10 \times 2.5 \text{ cm}$ (length \times width \times thickness) (Figure 5b). This geometry is recommended by the ISO 12571 standard [54] and Nordtest Protocol [55] for biobased

building materials. After molding, the mortars were kept in molds for 48 h and cured at room temperature of 23 ± 2 °C, with a relative humidity of $55 \pm 2\%$, until reaching 28 days of age.

Table 2. Bio-based earth mortar mixtures composition of adjusted constituents (kg/m^3).

| EMB | NS | BP | W_t | SP |
|------|---------|----|--------|-------|
| EMB0 | 1149.65 | - | 306.57 | 9.23 |
| EMB3 | 1070.15 | 15 | 319.06 | 13.85 |
| EMB6 | 990.65 | 30 | 328.31 | 13.85 |
| EMB9 | 911.15 | 45 | 337.57 | 13.85 |

NS—Natural sand; BP—Bamboo particles; W_t —Total water; SP—Superplasticizer.

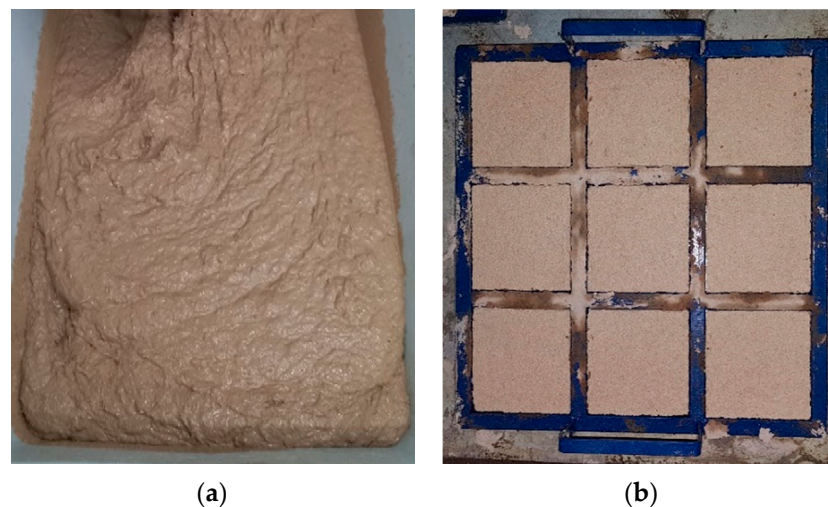


Figure 5. Earth-based bamboo mortar. (a) In its fresh state and (b) placed in molds.

2.3. Characterization of the Mortar

Before quantifying their physical and thermal properties, the samples were oven dried at 60 ± 2 °C until reaching the constancy of mass. Then the samples were cooled to room temperature in a desiccator containing silica gel. The bulk density (ρ_b) in the hardened state was determined according to the requirements of NBR 13280 [56]. To determine thermal conductivity (k) and specific heat (S_h), C-Therm equipment, model TCi, based on the modified transient plane source (MTPS) method, was employed. According to the equipment's manual [57], for porous materials it was necessary to use a contact agent (thermal grease) at the bottom surface of the sample (Figure 6a). Figure 6b shows the setup of the test. Due to the small contact area of the sensor and due to preferential orientation of the particles during casting (horizontally), it was decided to take readings at five surface regions, with 3 readings at each region, thus obtaining more representative values (average of all measurements).

In Table 3, the mean values obtained for the evaluated parameters are presented. The bulk density is an important property as it can correlate with many other properties of the composite material, such as thermal characteristics [18]. The studied mortars presented compressive strength in the range of 2.03 to 3.89 MPa, meeting the Brazilian requirements for plastering mortar. More details can be obtained in Paiva [58].

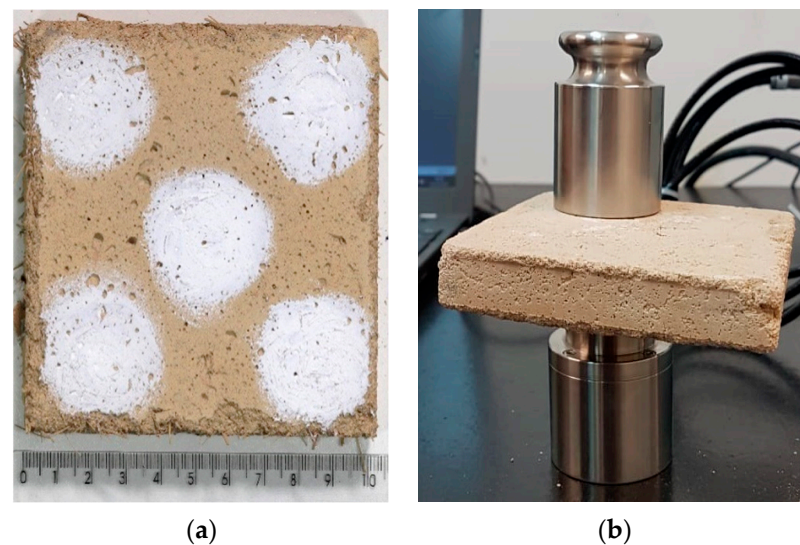


Figure 6. Thermal conductivity test. (a) Use of contact agent (thermal grease) at different positions on the sample and (b) sensor positioned on the sample.

Table 3. Physical and thermal properties.

| Mortar | Bulk Density (ρ_b) | Thermal Conductivity (k) | Specific Heat (S_H) |
|--------|----------------------------|--------------------------------------|---------------------------------------|
| | (kg/m^3) | ($\text{W}/\text{m}\cdot\text{K}$) | ($\text{J}/\text{kg}\cdot\text{K}$) |
| EMB0 | 1704.13 ± 1.26 | 0.62 ± 0.07 | 897.37 ± 13.26 |
| EMB3 | 1634.72 ± 0.50 | 0.55 ± 0.10 | 910.68 ± 14.86 |
| EMB6 | 1529.67 ± 0.71 | 0.49 ± 0.08 | 967.00 ± 15.82 |
| EMB9 | 1471.80 ± 0.77 | 0.43 ± 0.15 | 1003.34 ± 14.16 |
| CMS | 1465.48 ± 0.52 | 0.94 ± 0.10 | 1164.87 ± 25.59 |

It can be seen in Table 2 that some constituents underwent minor adjustments. However, for W_t and SP, these adjustments were not expressive, in volumetric terms, to produce important changes in physical properties. The natural sand (NS) had to be adjusted in order to enable the incorporation of bamboo particles (BP) and maintain a mixture volume of 1 m^3 . The significant difference between the bulk density values of these constituents ($\text{BP} = 500 \text{ kg}/\text{m}^3$ and $\text{NS} = 1600 \text{ kg}/\text{m}^3$) is highlighted. BP have a complex morphology and high multiscale porosity, characteristics common to all lignocellulosic materials [22], as can be seen in the SEM images in Figure 4. It is also noteworthy that the insertion of vegetable particles tends to trap air during the production of the mixtures [59]. The decrease in the mortar bulk density of up to 14% was influenced mainly by the addition of a high-volume fraction of BP. A tendency of a up to 31% value reduction in the thermal conductivity with the increase of the BP content was also observed in the study. These trends are in accordance with [60], which reports a relationship between bulk density and thermal conductivity of building insulating materials.

Liuzzi et al. [17] evaluated the thermal properties of four clay plasters with different percentages (4%, 6%, 8%, and 12%) of olive pruning fiber residues with an average size of 2 cm. He also observed a reduction in definition values ($1669\text{--}1409 \text{ kg}/\text{m}^3$) and thermal conductivity ($0.59\text{--}0.42 \text{ W}/\text{m}\cdot\text{K}$). As the percentage of olive fiber increased, for a specific heat capacity an inverse behavior was observed, that is, a specific heat increases with increasing fiber percentage ($849.57\text{--}958.91 \text{ J}/\text{kg}\cdot\text{K}$).

Palumbo et al. [15] evaluated the hygrothermal properties of earth plasters with three different percentages (0%, 1%, and 2%) of barley straw (2 mm), barley wool containing longer fibers, and corn grain granulate (1.0 mm). The referred authors also observed a reduction in bulk density and thermal conductivity with the increase in the fiber content

used. The authors obtained results where the matrix presented the highest values of bulk density and thermal conductivity (1848 kg/m³ and 1.40 W/m·K, respectively). After insertion of the fibers, these properties decreased, and the values obtained ranged between 1613–948 kg/m³ and 0.80–0.20 W/m·K, respectively.

The values obtained for a CMS are consistent with NBR 15220-2 [61], where a conventional mortar presents conductivity values of up to 1.15 W/m·K. When comparing the results of EMB9 with the CMS, the density did not show a significant change. However, when comparing the thermal conductivity results, a reduction of up to 52% was observed, which is directly related to the composition of the EMBs. Therefore, the results obtained in this research are consistent with the literature.

2.4. Life Cycle GHG Emissions Assessment

2.4.1. Definition of the Objective, Scope, and Functional Unit

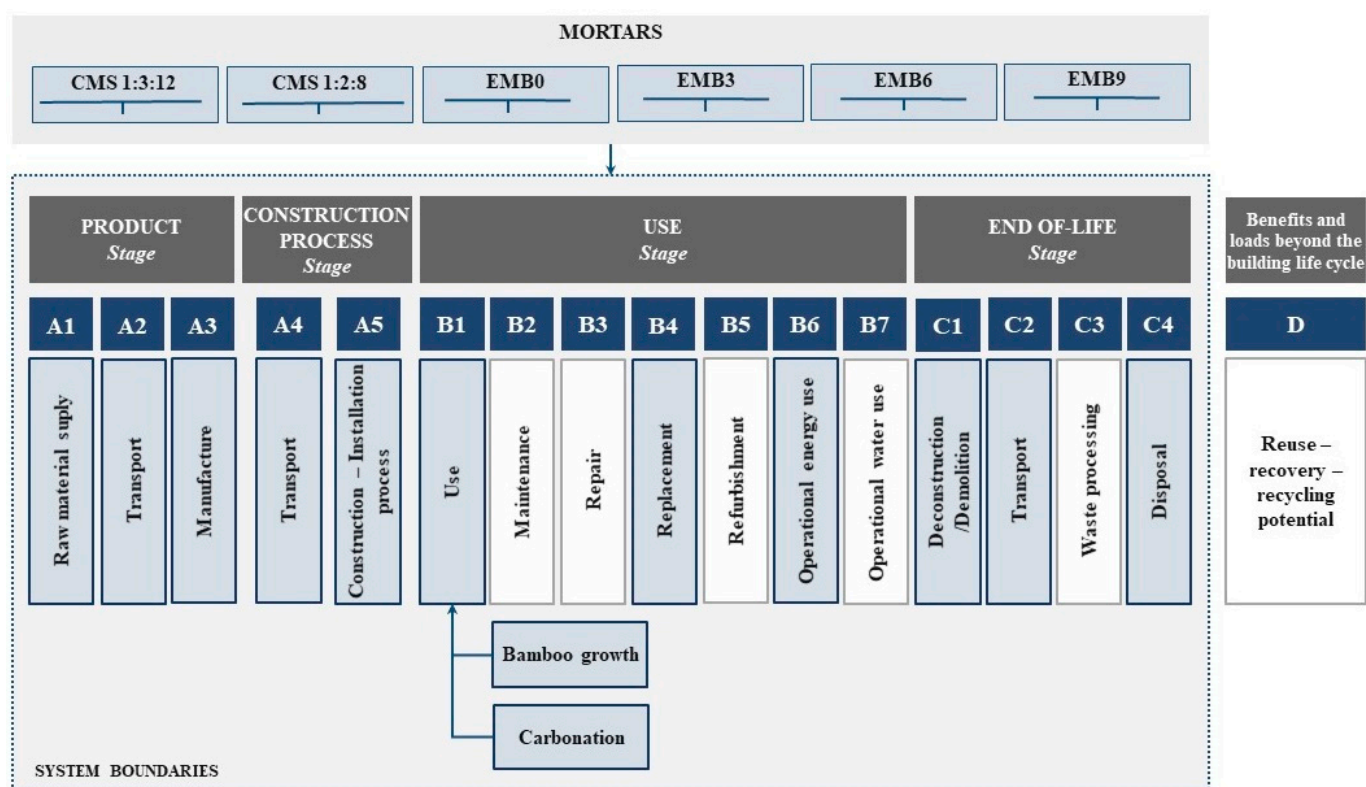
A life cycle GHG emissions assessment was carried out according to ISO 14040 [62] and EN 15804 [63]. The objective of this study was to compare the balance of GHG emissions (in kgCO₂-eq) in the life cycle of social housing covered with different mortars (EMB and CMS). Four EMBs were evaluated: without bamboo particles, and with 3%, 6%, and 9% of bamboo particles in volume. Two CMSs, commonly used in Brazilian buildings as plasters, were also evaluated, considering volumetric proportions of, respectively, cement to hydrated lime to sand of 1:2:8 and 1:3:12. This research can be classified as cradle-to-grave in scope [63] since the following stages are considered (Figure 7): raw materials' supply (A1), raw materials' transportation (A2), mortar production (A3), mortar transportation from factory to site (A4), mortar execution (A5), mortar use (B1), mortar replacement (B4), building operational energy consumption (B6) and end-of-life (C1–C4).

The functional unit (FU) was chosen as “a house with a service life of 50 years”. The house walls were covered with mortar of 5 cm or 3 cm thickness (2.5 cm or 1.5 cm on each side, respectively). The equivalent function was ensured, in terms of thermal performance, considering the same set-point into the house operation between the evaluated options. This is a widespread practice in LCA studies that compare solutions with distinct thermal characteristics [44,64].

In terms of durability, it was first assumed that EMBs and CMSs have the same service life. However, in the sensitivity analysis, different values of service life for EMBs were evaluated.

2.4.2. Life Cycle GHG Emissions Inventory

In the stage of the life cycle GHG emissions inventory, two types of data were used: primary data collected from the laboratory and secondary data, from the Ecoinvent v. 3.6 and scientific literature (presented in Supplementary Material, Table S1). This version of Ecoinvent already has datasets for the Brazilian context. Different stages were considered such as raw materials acquisition (A1), transportation (A2), considering the distances presented in Supplementary Material (Table S2), production in a factory (A3), transportation to the site, considering 200 km (A4), and the execution of the mortar (A5). The following materials are considered for the EMB production: earth, cement, fly ash, metakaolin, sand, bamboo particles, additives, and water; and for CMS: cement, hydrated lime, sand, and water. For the mortars replacement stage (B4), it was assumed that the last mortar is sent out to the nearest inert landfill (considering a distance of 50 km), and the novel mortar is transported from the factory to the building considering the same premises of stages A1–A4. In the use stage (B1), the biogenic carbon is quantified due to bamboo growth and the uptake of CO₂—due to the carbonation process. For the building operation (B6), only the electricity for the air conditioning is considered based on the results of the thermal-energy simulation. Finally, for the end-of-life stages, the demolition of mortars (C1), the transportation of waste (C2), and disposal in the nearest inert landfill (C4) are considered.



- Electricity grid mix factor—minimum— EF_{min} —0.130 kgCO₂-eq/kWh and maximum— EF_{max} —0.198 kgCO₂-eq/kWh based on González-Mahecha et al. [44];
- Wall's substrates—concrete wall (U-value of 4.4 W/m²·K) and concrete blocks masonry (U-value of 2.8 W/m²·K)
- Thickness of the plasters—3 and 5 cm;
- Two mixtures (in volume of cement: hydrated lime: sand) of cement-lime plasters—1:3:12 and 1:2:8.

2.5. Thermal-Energy Simulation

For the thermal-energy evaluation, the DesignBuilder software was employed considering the following cities with respective climate zones (according with Köppen-Geiger classification): (1) Curitiba: Cfb—Temperate/mesothermal climates—Oceanic climate; (2) Teresina: Aw—Tropical savanna climate with dry-winter; and (3) Rio de Janeiro: Am—Tropical monsoon climate. A standard project of a single-family social house in Brazil was adopted (Figure 8) with detailed information about design and construction according to Caldas et al. [64].

The chosen building had a typical residential typology for 3–4 people for Brazilian social housing also used in other studies [44,64,70,71]. Natural ventilation and air were considered in the simulation. The roof type used was composed of ceramic tiles supported by wood structure and with PVC ceiling without insulation.

Due to the air-conditioning, the electricity consumption was considered, according to the defined set-point temperatures (18 °C for heating and 23 °C for cooling based on previous studies [64,70]). Only the consumption related to cooling and heating was considered. However, it is important to say that thermal loads due to lighting and occupational and domestic appliances were measured since the referred loads influence the air-conditioning operation. The electricity consumption for heating was quantified only for a Temperate/mesothermal climate since this city (Curitiba) is the only one that uses an in-house heating operation.

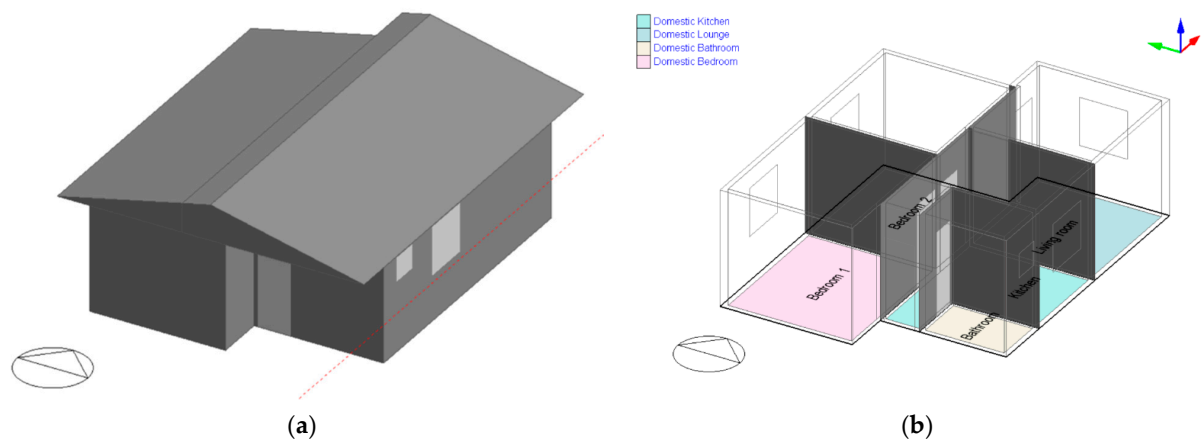


Figure 8. Model in the DesignBuilder software. (a) Social house project. (b) Thermal zones of the project.

As presented in the life cycle GHG emissions assessment sensitivity analysis, two total mortar thicknesses (5 cm and 3 cm) and two substrates were adopted in this research (Figure 9). The first substrate was a concrete wall with 10 cm of thickness and a worst thermal performance (U-value of 4.4 W/m²·K). The second was a 14 cm concrete block masonry with a better thermal performance (U-value of 3.0 W/m²·K).

Although in the past, concrete walls were not the most conventional technology used in Brazil. Their use has grown in recent years, mainly for the social housing segment, due to their high productivity and in spite of their unsatisfactory thermal performance [44]. Based on this statement, this technology and the conventional concrete blocks masonry were used in the study.

It is important to note that although wall insulation is a common practice in Northern countries, in Brazil it is not used, even in regions with colder climates. According to Hashemi [72], the use of internal wall insulation in tropical climates can lead to an overheating of the building. In some constructions, insulation is used in roofs but not in walls.

The mortars' thermal properties, measured in the laboratory, were used for modeling the walls in the DesignBuilder software. The thermal parameters (U-value and Thermal Capacity) are presented in Table 4. Based on these inputs, the annual electricity consumption of the house was obtained and presented in Supplementary Materials (Table S3).

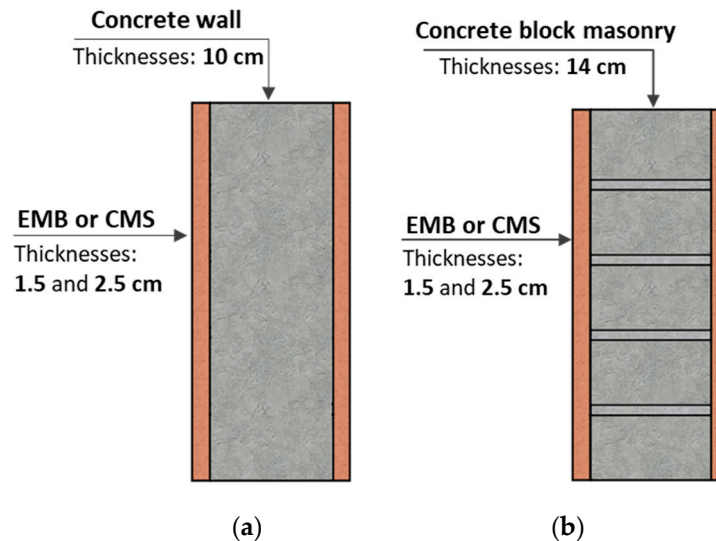


Figure 9. Schematic images of the analyzed walls with different substrates and thicknesses. (a) Concrete wall substrate. (b) concrete block masonry substrate.

Table 4. Thermal parameters for wall modeling in DesignBuilder.

| Wall Substrate | Options ¹ | Total Wall Thickness (mm) | U-Value (W/m ² ·K) | Thermal Capacity (kJ/m ² ·K) |
|------------------------|----------------------|---------------------------|-------------------------------|---|
| Concrete wall | EMB0—3 | 13 | 3.62 | 285.88 |
| | EMB3—3 | 13 | 3.55 | 284.66 |
| | EMB6—3 | 13 | 3.47 | 284.38 |
| | EMB9—3 | 13 | 3.36 | 284.30 |
| | CMS—3 | 13 | 3.86 | 291.21 |
| | EMB0—5 | 15 | 3.25 | 316.46 |
| | EMB3—5 | 15 | 3.14 | 314.44 |
| | EMB6—5 | 15 | 3.04 | 313.96 |
| | EMB9—5 | 15 | 2.91 | 313.84 |
| | CMS—5 | 15 | 3.56 | 325.35 |
| Concrete block masonry | EMB0—3 | 17 | 2.65 | 204.18 |
| | EMB3—3 | 17 | 2.61 | 202.96 |
| | EMB6—3 | 17 | 2.56 | 202.68 |
| | EMB9—3 | 17 | 2.51 | 202.60 |
| | CMS—3 | 17 | 2.77 | 209.51 |
| | EMB0—5 | 19 | 2.44 | 234.76 |
| | EMB3—5 | 19 | 2.38 | 232.74 |
| | EMB6—5 | 19 | 2.32 | 232.26 |
| | EMB9—5 | 19 | 2.24 | 232.14 |
| | CMS—5 | 19 | 2.62 | 243.65 |

¹ 3—plaster thickness of 3 cm. 5—plaster thickness of 5 cm.

3. Results

3.1. Total Life Cycle GHG Emissions

The total life cycle GHG emissions of all the cases are presented in Figures 10–13. Figures 10 and 11 show the total GHG emissions for each wall substrate (concrete wall and concrete block masonry) considering the minimum grid factor (EFmin), and Figures 12 and 13 for the electrical grid factor maximum (EFmax).

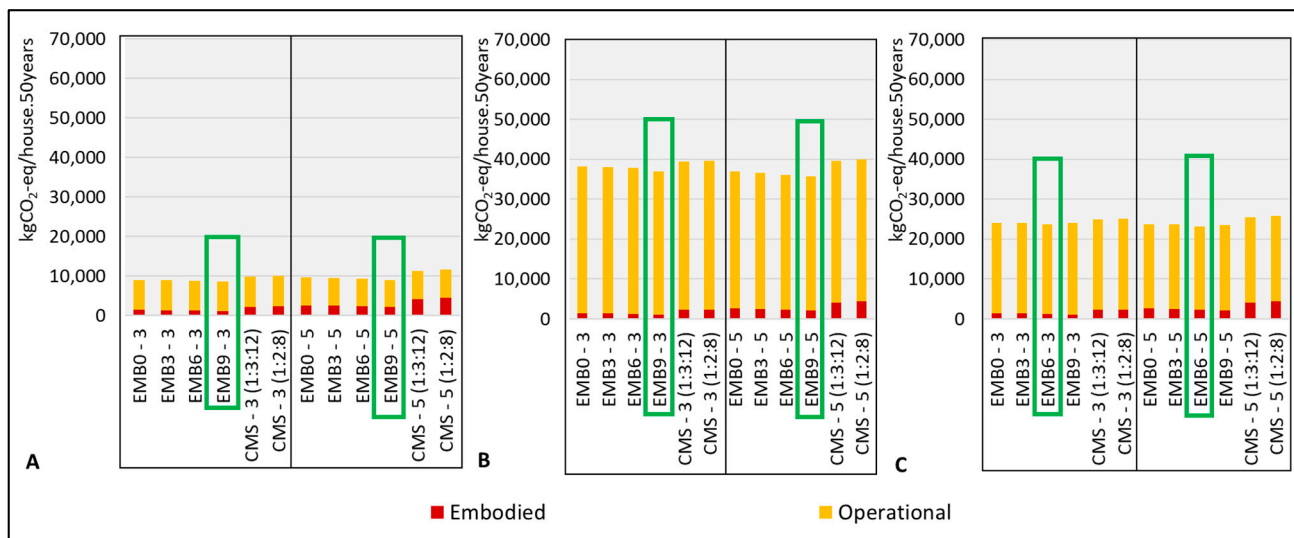


Figure 10. Total GHG emissions (embodied and operational) of all cases considering a concrete wall substrate and mortar thickness of 3 cm and 5 cm, respectively. EFmin=0.130 kgCO₂-eq/kWh. (A) Cfb—Temperate/mesothermal climate. (B) Aw—Tropical savanna climate with dry winter. (C) Am—Tropical monsoon climate. EMB—Earth mortar. CMS—Conventional, mortar. The green rectangles represent the option with smaller GHG emissions.

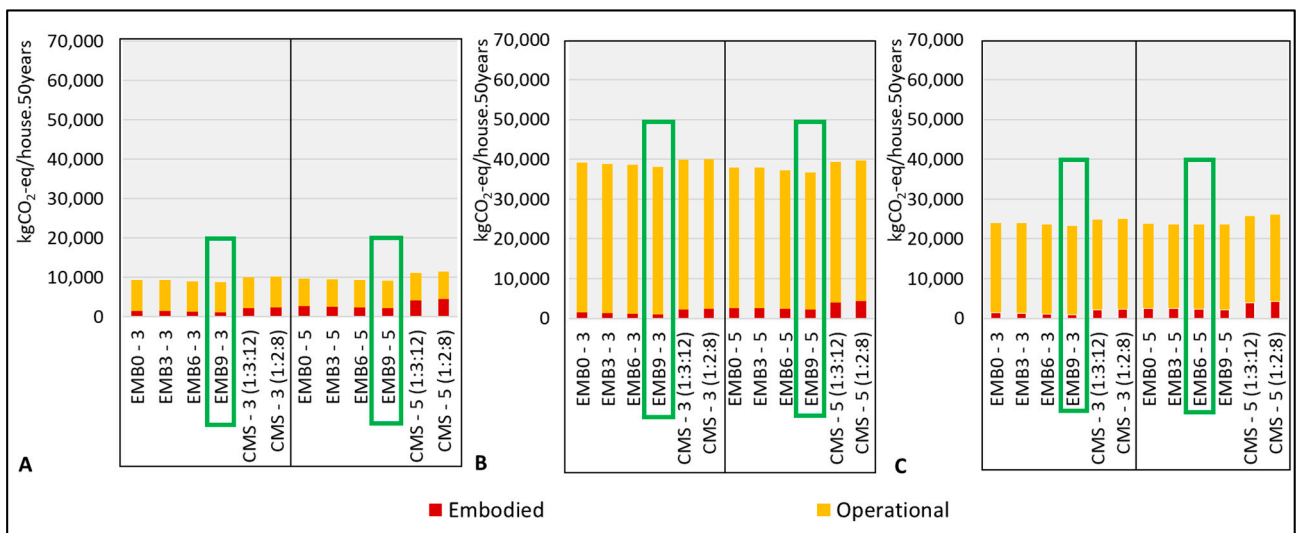


Figure 11. Total GHG emissions (embodied and operational) of all cases considering a concrete block masonry substrate and mortar thickness of 3 cm and 5 cm, respectively. EFmin=0.130 kgCO₂-eq/kWh. (A) Cfb—Temperate/mesothermal climate. (B) Aw—Tropical savanna climate with dry winter. (C) Am—Tropical monsoon climate. EMB—Earth mortar. CMS—Conventional, mortar. The green rectangles represent the option with smaller GHG emissions.

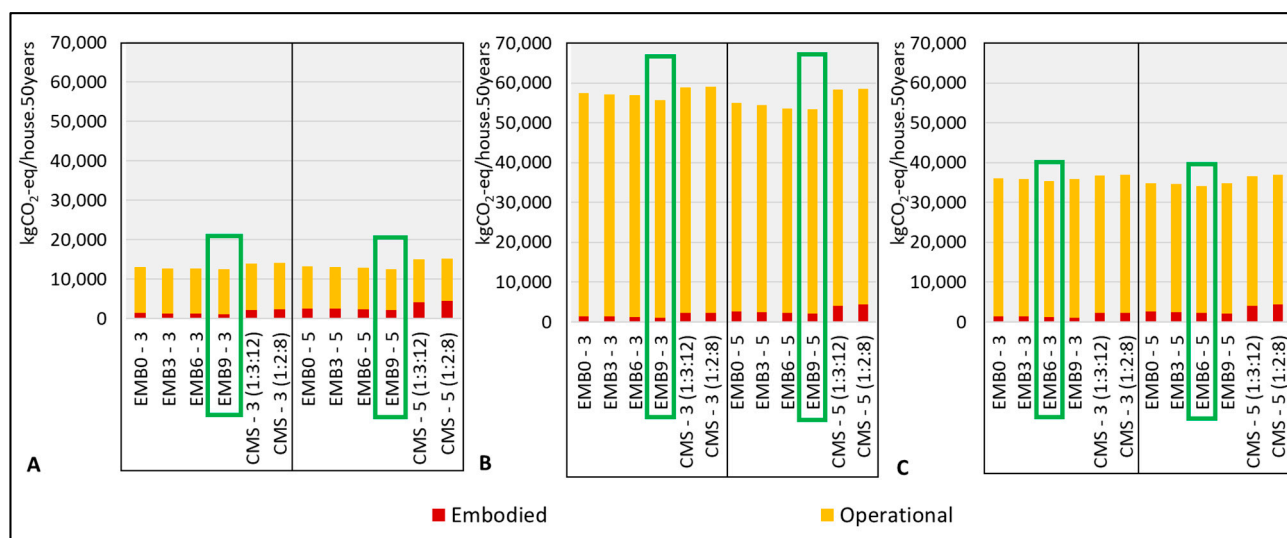


Figure 12. Total GHG emissions (embodied and operational) of all cases considering a concrete wall substrate and mortar thickness of 3 cm and 5 cm, respectively. $EF_{max}=0.198$ kgCO₂-eq/kWh. (A) Cfb—Temperate/mesothermal climate. (B) Aw—Tropical savanna climate with dry winter. (C) Am—Tropical monsoon climate. EMB—Earth mortar. CMS—Conventional, mortar. The green rectangles represent the option with smaller GHG emissions.

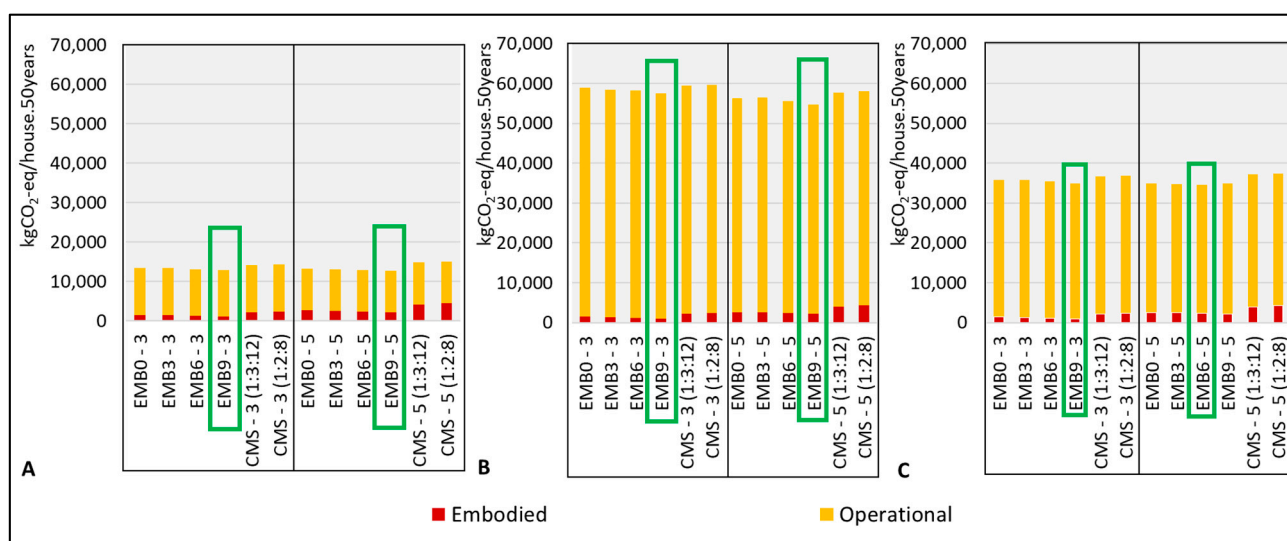


Figure 13. Total GHG emissions of all cases considering a concrete block masonry substrate and mortar thickness of 3 cm and 5 cm, respectively. $EF_{max}=0.198$ kgCO₂-eq/kWh. (A) Cfb—Temperate/mesothermal climate. (B) Aw—Tropical savanna climate with dry winter. (C) Am—Tropical monsoon climate. EMB—Earth mortar. CMS—Conventional, mortar. The green rectangles represent the option with smaller GHG emissions.

The life cycle GHG emissions ranged from 9 to 59 tCO₂-eq/house over 50 years for EMB9, EF_{min} with a 5 cm thickness in a temperate climate, and EMB0, EF_{max} with 3 cm thickness in a tropical savanna climate, respectively, considering the concrete wall substrate. It can be observed that the operational GHG emissions (yellow color) represent the highest total GHG emissions percentage, especially for tropical climates (Figures 10B,C, 11B,C, 12B,C and 13B,C) and EMBs cases. The EMB9 with a thickness of 5 cm and 3 cm presented the best choice for most scenarios, while the EMB0 was the worst option when comparing with the earth mortar options. The conventional cement-lime mortars (CMS) with a mixture proportion of 1:2:8 presented the worst results.

The EMB9 presented the greatest potential for GHG emissions reduction due to the high CO₂ storage, due to the high amount of bamboo aggregates. In addition, this option showed the best thermal performance due to the lower thermal conductivity and, consequently, the smaller U-value, which will result in less air conditioning consumption during the building's operational stage.

The kind of wall substrate, in this case, concrete wall or concrete block masonry, showed a slight influence on the total GHG emissions. Furthermore, the greater differences between the earth and conventional mortars were verified, for the substrate with the worst thermal performance (concrete wall) reaching 28%, for the temperate/mesothermal climate and EFmin. The EMBs showed better results for a temperate/mesothermal climate due to their better performance both for cooling and heating. This result shows the potential of EMBs, especially EMB9, for reducing operational energy and the life cycle of GHG emissions of a building located in tropical and temperate climates.

The electricity grid factor (EFmin and EFmax) value represented an important influence on total GHG emissions. For EFmax, the participation of the operational stage increased, especially for tropical savanna climate with dry winters, reaching 98% for EMB9—3 cm and concrete wall. Meanwhile, for EFmin, the operational stage reached the minimum value of 61% for temperate/mesothermal climate and CMS (1:2:8)—5 cm and concrete block masonry.

It is important to say that these results consider that the EMBs have the same service life as CMS. The results when half of the service life is considered for EMBs (or in other words, two replacements in the house service life) are presented in Supplementary Material (Figures S1–S4). For this scenario, the options presented similar results, with small differences (below 5%), for EMBs as the best options. If the fact that the EMBs have one-third of the service life of CMSs is considered, the EMBs turn to be more disadvantageous than CMSs. From these findings, it can be seen that the service life of mortars is a significant issue and should deserve special attention during the design of buildings, especially when earth is used as a building material. In terms of mortars application, it is necessary to specify adequate roofs with longer eaves and reliable floor and foundation system protection, with a special protection against water and moisture [42].

3.2. Embodied GHG Emissions

The embodied GHG emissions for each life cycle stage are presented in Figure 14 and specifically for each component of mortars in Figure 15.

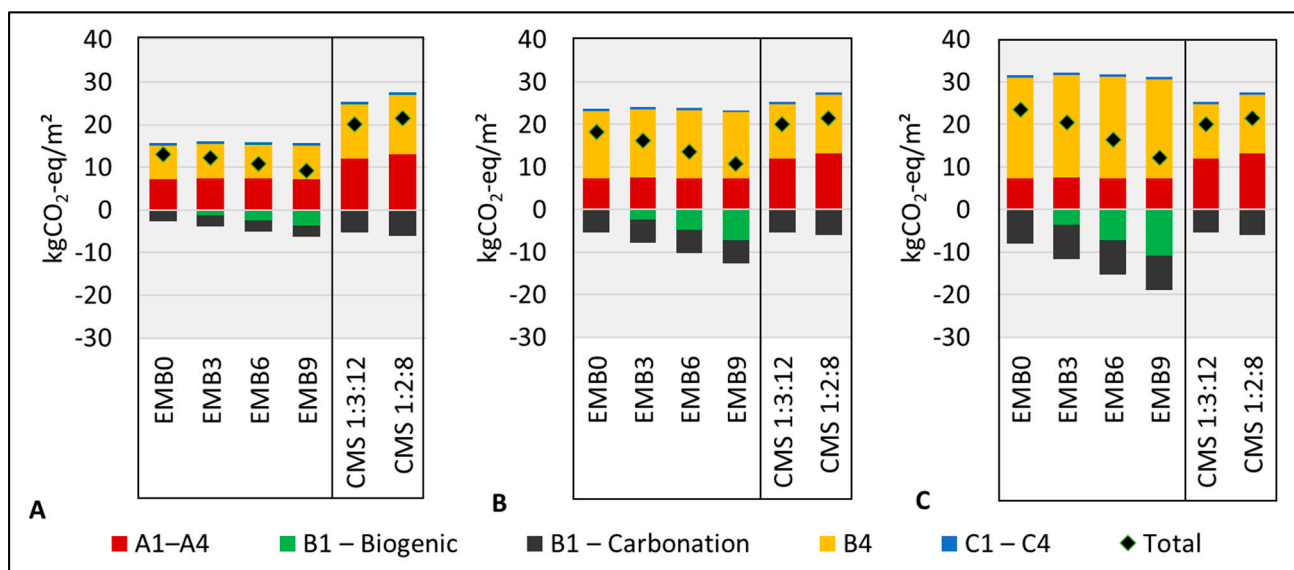


Figure 14. Embodied GHG emissions for life cycle stages considering a total thickness of 3 cm of mortar. (A) One replacement of earth mortar. (B) Two replacement of earth mortar. (C) Three replacement of earth mortar. EMB—Earth mortars. CMS—Conventional mortars.

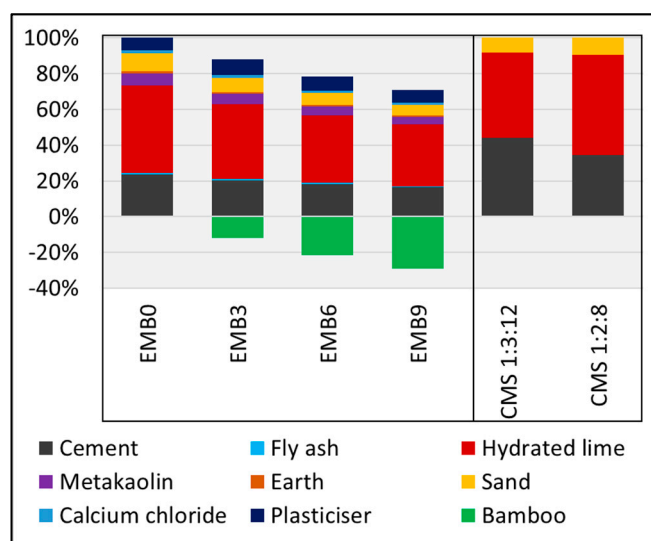


Figure 15. Embodied GHG emissions for each mortar in component level.

The production (A1–A4) and replacement (B4) stages represented the largest portion of embodied GHG emissions that agrees with the literature [43,64]. The carbonation, sequestration, and storage of CO₂ due to photosynthesis occurred in the usage stage (B1), entering the GHG balance as negative values. These two processes represented a considerable contribution to the GHG reduction. The increase of bamboo particles represented the increment of CO₂ stock, which is optimal in terms of GHG balance. The EMB9 presented the best result—valid, assuming that the bamboo particles will be stored permanently in the mortar.

The carbonation process, specifically in concrete structures, typically did not represent a significant contribution. Mortars that use lime in their formulation are especially important and should be measured in a life GHG emissions study, as already pointed out in other studies [53]. Additionally, it can be expected that since plasters were used in a minimal thickness, all the layers will be carbonated [53,68].

When a sensitivity analysis was carried out, it could be seen that the number of mortar replacements (yellow column in Figure 14) influenced greatly the final results. On the other hand, it could be observed that even considering the replacements of EMB9 and EMB6, those presented better results than the others due to the increase of biogenic carbon. It is important to say that this occurs because it was assumed that the bamboo aggregate and the biogenic carbon would remain stocked in the mortar's end-of-life due to the mineralization process caused by cementitious materials. For future research, this topic deserves special attention.

When the embodied carbon of mortar components was evaluated, it was perceived that the binders, principally hydrated lime and Portland cement, were the most GHG emission-intensive materials, which agrees with the literature related to mortars evaluation [13,42,53]. Calcium carbonate (CaCO₃) calcination is one of the most impactful processes due to the high amount of CO₂ released. Additionally, the fossil fuels, e.g., petroleum coke for Brazilian production, used for these material productions have an important contribution. The GHG emissions of metakaolin are also related to the calcination process, directly related to the type of fuel used [73].

Sand is responsible for the main portion of GHG emissions due to the extraction process that uses diesel-fueled machinery. In the current research, natural sand, extracted from a riverbed, was considered for the Brazilian context. The emissions of superplasticizer are influenced, especially by the production of organic compounds. Finally, earth and fly ash have almost negligible emissions since, for earth, just the extraction process produces GHG emissions, and for fly ash, just the grinding process was considered.

4. Discussion

Firstly, it is important to discuss the experimental findings. Based on the literature [60], there is a relationship between bulk density and thermal conductivity, with a tendency of up to 31% of value reduction with the increase of the bamboo particles content being also observed. The specific heat capacity (S_h) characterizes a material's capacity to store heat. Therefore, in the case of EMB9, results indicate that 1003.34 J are needed to raise the temperature by 1.0 K; whereas for EMB0, less than 897.37 J are needed to raise the temperature by 1.0 K. The latter would change its temperature faster and store more heat inside a building than a mortar with bamboo particles inserted. When analyzing the obtained results, an increase of up to 11% was observed, which is also related to the increase in the percentage of bamboo particles used.

These experimental results help to explain the lower life cycle GHG emissions of EMBs. The EMBs, especially EMB9, can be considered to be an adequate option in terms of a GHG investment. This term can be defined as a solution that decreases the operational GHG emissions with lower embodied GHG emissions. In the end, it is going to have lower total life cycle GHG emissions [43]. Additional bio-based and natural alternatives, such as bamboo bio-concrete [64], wooden [74–76], and earthen constructions [77–79], have already shown a similar performance.

It is important to say that most literature focus on the comparison between different wall configurations (changing the substrate and the use of insulation layers) [43]. However, there is a gap in the literature about the influence of plasters in terms of building energy efficiency, especially in the case of tropical and subtropical climates, where an insulation layer is not commonly used on walls. Although the plastering system is thin, it can bring some positive gains. Therefore, the entire wall system (substrate, insulation, and cladding) can be upgraded.

The EMB0 presented embodied GHG emissions for each m^2 of wall area ranging from 13 $kgCO_2$ -eq/ m^2 (with 3 cm thickness) to 24 $kgCO_2$ -eq/ m^2 (with 5 cm thickness) considering 1 replacement, while the EMB9 presented a range from 9 $kgCO_2$ -eq/ m^2 (with 3 cm) to 19 $kgCO_2$ -eq/ m^2 (with 5 cm) considering 1 replacement, which is higher than other, simpler, earth mortars used for plastering in the literature that showed values ranging from 3 $kgCO_2$ -eq/ m^2 to 7 $kgCO_2$ -eq/ m^2 [42]. This can occur due to several factors: mortar formulation, life cycle inventory used, scope (life cycle stages) and assumptions considered (e.g., transportation, service life, etc.), life cycle impact assessment method chosen, etc. [41,80,81]. On the other hand, cement and hydrated lime mortars present higher values, 20 $kgCO_2$ -eq/ m^2 (with 3 cm) to 39 $kgCO_2$ -eq/ m^2 (with 5 cm) and 35 $kgCO_2$ -eq/ m^2 to 50 $kgCO_2$ -eq/ m^2 , respectively, from the literature [53]. These numbers are important in terms of the definition of GHG emissions benchmarks, in this case, for the plastering element, and can be used for future public policies and low carbon targets [82].

Some items that severely affect the life cycle GHG emissions and overall performance of plastering are the thickness, the service life, and the executive processes. They deserve special attention during LCA modeling and design specification [13,42,53,83]. In order to have more reliable service life values of plasters, more experimental research data are required to serve as inputs for the LCA modeling, to have more accurate and assertive results, e.g., natural aging and/or accelerated aging for service life prediction of buildings' envelope [84,85].

Since hydrated lime was the hotspot of EMBs, in terms of GHG emissions, the next stage of this research should be to think of ways of decreasing its amount without compromising performance. One option already used in the mortar industry is the use of additional additives, such as air-entraining additives. Cirilo [52] found an almost 50% reduction in industrialized cement mortar GHG emissions compared with conventional mortar. This reduction was attributed to a significant replacement of the hydrated lime when a small amount of additive is used. For cement mortar production, the use of this additive is a mature technological solution, while for earth-based mortars, more research is required. The second hotspot is cement. Typically, the first strategy to decrease cement

GHG emissions is to replace it with supplementary cementitious material (SCM), such as fly ash, blast furnace slag, rice husk ash, and others [86–88]. However, previous research of Paiva et al. [89] shows that, depending on the amount of cement that is replaced for fly ash, the environmental performance is not satisfactory, and at the same time, the mechanical performance might be compromised. Therefore, the choice and amount of SCM that would replace cement should be considered with care.

Sand and earth extraction and production normally have low GHG emissions. However, this can change due to longer transportation distances [42]. In this case, the use of recycled concrete replacing sand and the use of excavated soil from constructions for earth replacement can be potential solutions and have already been studied [40,90].

The premise that the bamboo particles would be mineralized by the cementitious materials influences the final GHG balance, since part of them could decompose and release CO₂ and CH₄ to the atmosphere. However, most of the literature [64,68,73] regarding the use of cementitious materials mixed with bio-based materials considers a similar premise. Therefore, different options for the end-of-life stage regarding these materials should be evaluated in future studies.

Earth mortars, especially those with bio-based reinforcements, have additional benefits in terms of hydrothermal and air quality performance and are considered “breathing materials” [91,92]. However, these positive characteristics were not evaluated in this study. Our next challenge is to try and quantify how this extra benefit can be converted in terms of GHG emissions reduction and other environmental, social, and economic indicators.

In terms of the thermal simulation, some parameters that have not been evaluated, such as absorbance, setpoint of air conditioning, operation schedule, etc. [44], can influence the final results significantly. In terms of the climate data used in the modeling, a unique file, considering a typical reference year, has been contemplated. However, it is known that the climate is changing, and the global average temperature is increasing, which can influence the energy consumption for building artificial climatization. Studies [44,64,70] for similar climate conditions that consider the climate change effect in building operations have already been performed for Brazil and residential buildings and show that passive strategies and materials with better thermal performance tend to perform better than other lower-performance materials. EMBs are expected to be suitable for this scenario. However, for this verification, new simulations need to be carried out.

5. Conclusions

In this study, the life cycle GHG emissions (the carbon footprint) of different wall configurations were evaluated by comparing an earth mortar matrix with bamboo particles (EMB) with a conventional mortar (CMS). From the obtained results, it can be concluded that:

- The insertion of different percentages of bamboo particles in the beneficial matrix provides a bulk density reduction, thermal conductivity, and an increase in specific heat as in earth mortar matrix thermal properties;
- The EMB shows a smaller carbon footprint than CMS, even when considering different replacement scenarios;
- The use of EMB improves the buildings’ thermal performance with lower energy consumption and GHG emissions;
- The increase of bamboo particles in EMB mixtures decreases its carbon footprint due to a higher carbon stock and a better thermal performance during building operation;
- The greater differences between EMB and CMS occur for the coldest city—Curitiba (temperate/mesothermal climates)—an influence of the higher participation of embodied GHG emissions;
- The number of mortar replacements severely affects the final results.

In addition, it is necessary to describe the main limitations of this study: some of the used LCA databases are not adapted to the Brazilian context and can influence the final results; other parameters can affect the thermal energy simulation, such as building sched-

ule occupation, set point temperature, solar absorption among others. The assumption that the bamboo particles would be mineralized by the cementitious materials influences the final GHG balance, since some bamboo particles could decompose and emit CO₂ and CH₄. However, these limitations do not invalidate the results. For future research, it is recommended to overcome some of these limitations and increase the robustness of the study by analyzing other parameters (as sensitivity analysis), such as an alternative type of end-of-life and other environmental impacts of these earth-engineered mortars.

Supplementary Materials: The following are available online at <https://www.mdpi.com/article/10.3390/su131810429/s1>, Table S1: Datasets used in the Life cycle GHG emissions inventory, Table S2: Transportation distances, Table S3: Annual electricity consumption for building, Figure S1: Total GHG emissions (embodied and operational) of all cases considering a concrete wall substrate and mortar thickness of 3 cm and 5 cm, respectively. EF_{min}—0.130 kgCO₂-eq/kWh. (A) Cfb—Temperate/mesothermal climate. (B) Aw—Tropical savanna climate with dry winter. (C) Am—Tropical monsoon climate. EMB—Earth mortar. CMS—Conventional, mortar. The green rectangles represent the option with smaller GHG emissions, Figure S2: Total GHG emissions (embodied and operational) of all cases considering a concrete block masonry substrate and mortar thickness of 3 cm and 5 cm, respectively. EF_{min}—0.130 kgCO₂-eq/kWh. (A) Cfb—Temperate/mesothermal climate. (B) Aw—Tropical savanna climate with dry winter. (C) Am—Tropical monsoon climate. EMB—Earth mortar. CMS—Conventional, mortar. The green rectangles represent the option with smaller GHG emissions, Figure S3: Total GHG emissions (embodied and operational) of all cases considering a concrete wall substrate and mortar thickness of 3 cm and 5 cm, respectively. EF_{max}—0.198 kgCO₂-eq/kWh. (A) Cfb—Temperate/mesothermal climate. (B) Aw—Tropical savanna climate with dry winter. (C) Am—Tropical monsoon climate. EMB—Earth mortar. CMS—Conventional, mortar. The green rectangles represent the option with smaller GHG emissions. Figure S4: Total GHG emissions of all cases considering a concrete block masonry and mortar thickness of 3 cm and 5 cm, respectively. EF_{max}—0.198 kgCO₂-eq/kWh. (A) Cfb—Temperate/mesothermal climate. (B) Aw—Tropical savanna climate with dry winter. (C) Am—Tropical monsoon climate. EMB—Earth mortar. CMS—Conventional, mortar. The green rectangles represent the option with smaller GHG emissions.

Author Contributions: Conceptualization, R.d.L.M.P. and L.R.C.; methodology, R.d.L.M.P., L.R.C. and A.P.d.S.M. software, L.R.C., R.d.L.M.P., P.B.d.S. and G.F.d.O.; validation, L.R.C., R.d.L.M.P., P.B.d.S. and G.F.d.O.; formal analysis, R.d.L.M.P. and L.R.C.; investigation, L.R.C., R.d.L.M.P., P.B.d.S. and G.F.d.O.; data curation, L.R.C., R.d.L.M.P., P.B.d.S. and G.F.d.O.; writing—original draft preparation, R.d.L.M.P., L.R.C. and A.P.d.S.M.; writing—review and editing, R.d.L.M.P., L.R.C., A.P.d.S.M. and R.D.T.F.; visualization, R.d.L.M.P., L.R.C., A.P.d.S.M. and R.D.T.F.; supervision and mentoring, R.D.T.F.; project coordination, R.D.T.F. All authors have read and agreed to the published version of the manuscript.

Funding: This study was financed in part by Conselho Nacional de Desenvolvimento Científico e Tecnológico (CNPq) and by the Coordenação de Aperfeiçoamento de Pessoal de Nível Superior—Brasil (CAPES)—Finance Code 001.

Institutional Review Board Statement: Not applicable.

Informed Consent Statement: Not applicable.

Data Availability Statement: Not applicable.

Acknowledgments: It is a pleasure to acknowledge the financial support for this investigation provided by the Brazilian agencies CNPq and CAPES. The authors also express their gratitude to the editor and anonymous reviewers for comments and suggestions. The authors would like to thank Oscar Reales, Yasmin Mendonça, and Camila Carreira for their help with some experiments and data collection. They also would like to acknowledge researchers Francesco Pittau and Guillaume Habert from ETH Zürich, Institut für Bau- und Infrastrukturmanagement, Chair of Sustainable Construction, for the previous discussion about the theme of LCA and bio-based materials. Finally, we want to thank Katerina Dimitrova and Ursula Ghavami for the language review.

Conflicts of Interest: The authors declare no conflict of interest.

References

1. UNEP—United Nations Environment Programme. *2020 Global Status Report for Buildings and Construction: Towards a Zero-Emission, Efficient and Resilient Buildings and Construction Sector*; UNEP: Nairobi, Kenya, 2020.
2. UNEP—United Nations Environment Programme. *2019 Global Status Report for Buildings and Construction. Towards a Zero-Emissions, Efficient and Resilient Buildings and Construction Sector*; UNEP: Nairobi, Kenya, 2019; p. 41, ISBN 978-92-807-3768-4. Available online: <https://www.unep.org/resources/publication/2019-global-status-report-buildings-and-construction-sector> (accessed on 20 July 2021).
3. IPCC —Intergovernmental Panel on Climate Change. *Climate Change 2014: Mitigation of Climate Change. Contribution of Working Group III Contribution to the Fifth Assessment Report of the Intergovernmental Panel on Climate Change*; IPCC: Cambridge, UK, 2014; Volume 38.
4. Cellura, M.; Ciulla, G.; Guarino, F.; Longo, S. Redesign of a rural building in a heritage site in Italy: Towards the Net Zero energy target. *Buildings* **2017**, *7*, 68. [[CrossRef](#)]
5. Baglivo, C. Dynamic evaluation of the effects of climate change on the energy renovation of a school in a mediterranean climate. *Sustainability* **2021**, *13*, 6375. [[CrossRef](#)]
6. Fang, Z.; Li, N.; Li, B.; Luo, G.; Huang, Y. The effect of building envelope insulation on cooling energy consumption in summer. *Energy Build.* **2014**, *77*, 197–205. [[CrossRef](#)]
7. Del Rosario, P.; Palumbo, E.; Traverso, M. Environmental product declarations as data source for the environmental assessment of buildings in the context of level(S) and dgnb: How feasible is their adoption? *Sustainability* **2021**, *13*, 6143. [[CrossRef](#)]
8. Michalak, J.; Czernik, S.; Marcinek, M.; Michalowski, B. Environmental burdens of external thermal insulation systems. Expanded polystyrene vs. mineral wool: Case study from Poland. *Sustainability* **2020**, *12*, 4532. [[CrossRef](#)]
9. Sattler, S.; Österreicher, D. Assessment of sustainable construction measures in building refurbishment-life cycle comparison of conventional and Multi-Active Façade systems in a social housing complex. *Sustainability* **2019**, *11*, 4487. [[CrossRef](#)]
10. Ashour, T.; Wieland, H.; Georg, H.; Bockisch, F.J.; Wu, W. The influence of natural reinforcement fibres on insulation values of earth plaster for straw bale buildings. *Mater. Des.* **2010**, *31*, 4676–4685. [[CrossRef](#)]
11. Binici, H.; Aksogan, O.; Bodur, M.N.; Akca, E.; Kapur, S. Thermal isolation and mechanical properties of fibre reinforced mud bricks as wall materials. *Constr. Build. Mater.* **2007**, *21*, 901–906. [[CrossRef](#)]
12. Colinart, T.; Vineslas, T.; Lenormand, H.; De Menibus, A.H.; Hamard, E.; Lecompte, T. Hygrothermal properties of light-earth building materials. *J. Build. Eng.* **2020**, *29*, 101134. [[CrossRef](#)]
13. Melià, P.; Ruggieri, G.; Sabbadini, S.; Dotelli, G. Environmental impacts of natural and conventional building materials: A case study on earth plasters. *J. Clean. Prod.* **2014**, *80*, 179–186. [[CrossRef](#)]
14. Gomes, M.I.; Faria, P.; Gonçalves, T.D. Earth-based mortars for repair and protection of rammed earth walls. Stabilization with mineral binders and fibers. *J. Clean. Prod.* **2018**, *172*, 2401–2414. [[CrossRef](#)]
15. Palumbo, M.; McGregor, F.; Heath, A.; Walker, P. The influence of two crop by-products on the hygrothermal properties of earth plasters. *Build. Environ.* **2016**, *105*, 245–252. [[CrossRef](#)]
16. Santos, T.; Faria, P.; Silva, V. Can an earth plaster be efficient when applied on different masonries? *J. Build. Eng.* **2019**, *23*, 314–323. [[CrossRef](#)]
17. Liuzzi, S.; Rubino, C.; Stefanizzi, P.; Petrella, A.; Boghetich, A.; Casavola, C.; Pappalettera, G. Hygrothermal properties of clayey plasters with olive fibers. *Constr. Build. Mater.* **2018**, *158*, 24–32. [[CrossRef](#)]
18. Laborel-Préneron, A.; Aubert, J.E.; Magniont, C.; Tribout, C.; Bertron, A. Plant aggregates and fibers in earth construction materials: A review. *Constr. Build. Mater.* **2016**, *111*, 719–734. [[CrossRef](#)]
19. Asdrubali, F.; D’Alessandro, F.; Schiavoni, S. A review of unconventional sustainable building insulation materials. *Sustain. Mater. Technol.* **2015**, *4*, 1–17. [[CrossRef](#)]
20. Luhar, S.; Cheng, T.W.; Luhar, I. Incorporation of natural waste from agricultural and aquacultural farming as supplementary materials with green concrete: A review. *Compos. Part B Eng.* **2019**, *175*, 107076. [[CrossRef](#)]
21. Amziane, S.; Sonebi, M. Overview on bio-based building material made with plant aggregate Overview on bio-based building material made with plant aggregate. *RILEM Tech. Lett.* **2016**, *1*, 31–38. [[CrossRef](#)]
22. Amziane, S.; Collet, F. *Bio-Aggregates Based Building Materials: State-of-the-Art Report of the RILEM Technical Committee 236-BBM*; Springer: Heidelberg, Germany, 2017; Volume 23, ISBN 978-94-024-1030-3.
23. Caldas, L.R.; Saraiva, A.B.; Lucena, A.F.P.; Da Gloria, M.Y.; Santos, A.S.; Filho, R.D.T. Building materials in a circular economy: The case of wood waste as CO₂-sink in bio concrete. *Resour. Conserv. Recycl.* **2021**, *166*. [[CrossRef](#)]
24. Grazieschi, G.; Asdrubali, F.; Thomas, G. Embodied energy and carbon of building insulating materials: A critical review. *Clean. Environ. Syst.* **2021**, *2*, 100032. [[CrossRef](#)]
25. Aste, N.; Della, S.; Cinzia, T.; Rajendra, T.; Adhikari, S.; Rossi, C. *Models for Sustainable Development in Emerging African Countries*; Springer International Publishing: Heidelberg, Germany, 2020; ISBN 9783030333225.
26. Faria, P. Argamassas de terra e cal—Características e campos de aplicação. In Proceedings of the V Jorn. FICAL—Fórum Ibérico Da Cal, Lisboa, Portugal, 23–25 May 2016; pp. 277–286, ISBN 978-972-49-2281-2.
27. Parrella, V.F.; Molari, L. Building retrofitting system based on bamboo-steel hybrid exoskeleton structures: A case study. *Sustainability* **2021**, *13*, 5984. [[CrossRef](#)]

28. Agliata, R.; Marino, A.; Mollo, L.; Pariso, P. Historic building energy audit and retrofit simulation with hemp-lime plaster-A case study. *Sustainability* **2020**, *12*, 4620. [[CrossRef](#)]
29. Caniato, M.; D'Amore, G.K.O.; Kaspar, J.; Gasparella, A. Sound absorption performance of sustainable foam materials: Application of analytical and numerical tools for the optimization of forecasting models. *Appl. Acoust.* **2020**, *161*, 107166. [[CrossRef](#)]
30. Caniato, M.; Cozzarini, L.; Schmid, C.; Gasparella, A. Acoustic and thermal characterization of a novel sustainable material incorporating recycled microplastic waste. *Sustain. Mater. Technol.* **2021**, *28*, e00274. [[CrossRef](#)]
31. Binici, H.; Eken, M.; Dolaz, M.; Aksogan, O.; Kara, M. An environmentally friendly thermal insulation material from sunflower stalk, textile waste and stubble fibres. *Constr. Build. Mater.* **2014**, *51*, 24–33. [[CrossRef](#)]
32. Quiñones-Bolaños, E.; Gómez-Oviedo, M.; Mouthon-Bello, J.; Sierra-Vitola, L.; Berardi, U.; Bustillo-Lecompte, C. Potential use of coconut fibre modified mortars to enhance thermal comfort in low-income housing. *J. Environ. Manag.* **2021**, *277*, 111503. [[CrossRef](#)] [[PubMed](#)]
33. Salzer, C.; Wallbaum, H.; Ostermeyer, Y.; Kono, J. Environmental performance of social housing in emerging economies: Life cycle assessment of conventional and alternative construction methods in the Philippines. *Int. J. Life Cycle Assess* **2017**, *22*, 1785–1801. [[CrossRef](#)]
34. da Gloria, M.Y.R.; Andreola, V.M.; dos Santos, D.O.J.; Pepe, M.; Toledo Filho, R.D. A comprehensive approach for designing workable bio-based cementitious composites. *J. Build. Eng.* **2021**, *34*, 101696. [[CrossRef](#)]
35. Liu, P.; Zhou, Q.; Jiang, N.; Zhang, H.; Tian, J. Fundamental research on tensile properties of phyllostachys bamboo. *Results Mater.* **2020**, *7*, 100076. [[CrossRef](#)]
36. Bahtiar, E.T.; Imanullah, A.P.; Hermawan, D.; Nugroho, N. Abdurachman Structural grading of three sympodial bamboo culms (Hitam, Andong, and Tali) subjected to axial compressive load. *Eng. Struct.* **2019**, *181*, 233–245. [[CrossRef](#)]
37. Zea Escamilla, E.; Habert, G. Environmental impacts of bamboo-based construction materials representing global production diversity. *J. Clean. Prod.* **2014**, *69*, 117–127. [[CrossRef](#)]
38. Cabeza, L.F.; Rincón, L.; Vilariño, V.; Pérez, G.; Castell, A. Life cycle assessment (LCA) and life cycle energy analysis (LCEA) of buildings and the building sector: A review. *Renew. Sustain. Energy Rev.* **2014**, *29*, 394–416. [[CrossRef](#)]
39. Chau, C.K.; Leung, T.M.; Ng, W.Y. A review on Life Cycle Assessment, Life Cycle Energy Assessment and Life Cycle Carbon Emissions Assessment on buildings. *Appl. Energy* **2015**, *143*, 395–413. [[CrossRef](#)]
40. Grabois, T.M.; Caldas, L.R. An Experimental and Environmental Evaluation of Mortars with Recycled Demolition Waste from a Hospital Implosion in Rio de Janeiro. *Sustainability* **2020**, *12*, 8945. [[CrossRef](#)]
41. Santos, T.; Almeida, J.; Silvestre, J.D.; Faria, P. Life cycle assessment of mortars: A review on technical potential and drawbacks. *Constr. Build. Mater.* **2021**, *288*, 123069. [[CrossRef](#)]
42. Caldas, L.R.; Paiva, R.D.L.M.; de Martins, A.P.S.; Toledo Filho, R.D. Argamassas De Terra Versus Convencionais: Avaliação Do Desempenho Ambiental Considerando O Ciclo De Vida. *Mix Sustentável* **2020**, *6*, 115–128. [[CrossRef](#)]
43. Röck, M.; Saade, M.R.M.; Balouktsi, M.; Rasmussen, F.N.; Birgisdottir, H.; Frischknecht, R.; Habert, G.; Lützkendorf, T. Embodied GHG emissions of buildings—The hidden challenge for effective climate change mitigation. *Appl. Energy* **2019**, *258*, 114107. [[CrossRef](#)]
44. González Mahecha, R.E.; Caldas, L.R.; Garaffa, R.; Lucena, A.F.P.; Szklo, A.; Toledo Filho, R.D. Constructive systems for social housing deployment in developing countries: A case study using dynamic life cycle carbon assessment and cost analysis in Brazil. *Energy Build.* **2020**, *227*, 110395. [[CrossRef](#)]
45. Associação Brasileira de Normas Técnicas. *Soil Samples—Preparation for compaction and Characterization Tests*; NBR. 6457; ABNT: Rio de Janeiro, Brazil, 1986.
46. Associação Brasileira de Normas Técnicas. *Aggregates—Sieve Analysis of Fine and Coarse Aggregates*; NBR NM. 248; ABNT: Rio de Janeiro, Brazil, 2003.
47. Restrepo, A.; Becerra, R.; Tibaquirá, J.E.G. Energetic and carbon footprint analysis in manufacturing process of bamboo boards in Colombia. *J. Clean. Prod.* **2016**, *126*, 563–571. [[CrossRef](#)]
48. Associação Brasileira de Normas Técnicas. *Fine Aggregate—Determination of the Bulk Specific Gravity and Apparent Specific Gravity*; NBR NM 52; ABNT: Rio de Janeiro, Brazil, 2009.
49. Associação Brasileira de Normas Técnicas. *Coarse Aggregate—Determination of Total Moisture Content—Test Method*; NBR 9939; ABNT: Rio de Janeiro, Brazil, 2011.
50. American Association of State and Highway Transportation Officials. *Method of Test for Determining Aggregate Shape Properties by Means of Digital Image Analysis*; TP 81; AASHTO: Washington, DC, USA, 2017.
51. Masad, E.A. *Aggregate imaging system (AIMS): Basics and applications. Performing Organization Code Project 5-1707-01*; Type Rep. Period Cover. Unclassif.; Texas Transportation Institute, Texas A & M University System: College Station, TX, USA, 2005; p. 58.
52. Cirilo, F.; Melo, A.T.S. *Comparativo de Desempenho Ambiental entre Argamassa Industrializada e Argamassa Virada em Obra*; VI Congresso Brasileiro sobre Gestão do Ciclo de Vida: Brasília, Brazil, 2018; p. 6.
53. Caldas, L.R.; Carvalho, M.T.M.; Toledo Filho, R.D. Avaliação de estratégias para a mitigação dos impactos ambientais de revestimentos argamassados no Brasil. *Ambient. Construído* **2020**, *20*, 343–362. [[CrossRef](#)]
54. ISO. 12571. *Hygrothermal Performance of Building Materials and Products—Determination of Hygroscopic Sorption Properties*; International Organization for Standardization: Geneva, Switzerland, 2013; p. 18.

55. Rode, C.; Peuhkuri, R.H.; Hansen, K.K.; Time, B.; Svennberg, K.; Arfvidsson, J.; Ojanen, T. NORDTEST Project on Moisture Buffer Value of Materials. In Proceedings of the AIVC Conference ‘Energy Performance Regulation’: Ventilation in Relation to the Energy Performance of Buildings, Brussels, Belgium, 1 January 2005; pp. 47–52.
56. Associação Brasileira de Normas Técnicas. *Mortars Applied on Walls and Ceilings—Determination of the Specific Gravity in the Hardened Stage*; NBR. 13280; ABNT: Rio de Janeiro, Brazil, 2005.
57. C-THERM TECHNOLOGIES. *Simplifying Thermal Conductivity (k)—Equipment Manual*. Available online: <https://ctherm.com/thermal-conductivity-instruments/tci-thermal-conductivity-analyzer/> (accessed on 30 July 2021).
58. Paiva, R.L.M. Hygrothermal Properties, Biological Durability and Life Cycle Assessment of Earth Mortars with Bamboo Particles. Ph.D. Thesis, Federal University of Rio de Janeiro/PEC/COPPE, Rio de Janeiro, Brazil, 2020. Document in Portuguese. pp. 1–176.
59. Savastano, H.J. Materiais à Base de Cimento Reforçado Com Fibra Vegetal: Reciclagem de Resíduos Para a Construção de Baixo Custo. Ph.D. Thesis, University of São Paulo, São Paulo, Brazil, 2000. Document in Portuguese. pp. 1–152.
60. Hung Anh, L.D.; Pásztor, Z. An overview of factors influencing thermal conductivity of building insulation materials. *J. Build. Eng.* **2021**, *44*, 102604. [[CrossRef](#)]
61. Associação Brasileira de Normas Técnicas. *Thermal Performance in Buildings Part 2: Calculation Methods of Thermal Transmittance, Thermal Capacity, Thermal Delay and Solar Heat Factor of Elements and Components of Buildings*; NBR. 15220-2; ABNT: Rio de Janeiro, Brazil, 2005.
62. ISO. 14040. *Environmental Management—Life Cycle Assessment—Principles and Framework*; European Committee for Standardization: Brussels, Belgium, 2006; p. 20. ISBN 0 580 48993 0.
63. EN CEN. 15804:2012 + A2:2019—*Sustainability of Construction Works—Environmental Product Declarations—Core Rules for the Product Category of Construction Products*; European Committee for Standardization: Brussels, Belgium, 2012; p. 72.
64. Caldas, L.R.; Saraiva, A.B.; Andreola, V.M.; Dias Toledo Filho, R. Bamboo bio-concrete as an alternative for buildings’ climate change mitigation and adaptation. *Constr. Build. Mater.* **2020**, *263*, 120652. [[CrossRef](#)]
65. PD CEN ISO/TS 14067. *Greenhouse Gases—Carbon Footprint of Products—Requirements and Guidelines for Quantification and Communication*; European Committee for Standardization: Brussels, Belgium, 2014; p. 52.
66. Dolezal, F.; Hill, C.A.S.; Escamilla, E.Z. Comparative assessment for biogenic carbon accounting methods in carbon footprint of products: A review study for construction materials based on forest products. *iForest* **2017**, *10*, 815–823. [[CrossRef](#)]
67. Guest, G.; Cherubini, F.; Strømman, A.H. Global Warming Potential of Carbon Dioxide Emissions from Biomass Stored in the Anthroposphere and Used for Bioenergy at End of Life. *J. Ind. Ecol.* **2012**, *17*, 20–30. [[CrossRef](#)]
68. Pittau, F.; Krause, F.; Lumia, G.; Habert, G. Fast-growing bio-based materials as an opportunity for storing carbon in exterior walls. *Build. Environ.* **2018**, *129*, 117–129. [[CrossRef](#)]
69. Lagerblad, B. *Carbon Dioxide Uptake during Concrete Life Cycle: State of the Art*; Swedish Cement and Concrete Research Institute: Stockholm, Sweden, 2005; ISBN 91-976070-0-2.
70. Invidiata, A.; Ghisi, E. Impact of climate change on heating and cooling energy demand in houses in Brazil. *Energy Build.* **2016**, *130*, 20–32. [[CrossRef](#)]
71. Triana, M.A.; Lamberts, R.; Sassi, P. Should we consider climate change for Brazilian social housing? Assessment of energy efficiency adaptation measures. *Energy Build.* **2018**, *158*, 1379–1392. [[CrossRef](#)]
72. Hashemi, A. ScienceDirect Effects of thermal insulation on thermal comfort in low-income tropical housing. *Energy Procedia* **2017**, *134*, 815–824. [[CrossRef](#)]
73. Rosse, L.; Yassin, M.; Da Gloria, R.; Pittau, F.; Maria, V.; Habert, G.; Toledo, R.D. Environmental impact assessment of wood bio-concretes: Evaluation of the influence of different supplementary cementitious materials. *Constr. Build. Mater.* **2021**, *268*, 121146. [[CrossRef](#)]
74. Wang, Y.; Fukuda, H. Timber Chips as the Insulation Material for Energy Saving in Prefabricated Offices. *Sustainability* **2016**, *8*, 587. [[CrossRef](#)]
75. Margani, G.; Evola, G.; Tardo, C.; Marino, E.M. Energy, Seismic, and Architectural Renovation of RC Framed Buildings with Prefabricated Timber Panels. *Sustainability* **2020**, *12*, 4845. [[CrossRef](#)]
76. Valluzzi, M.R.; Saler, E.; Vignato, A.; Salvalaggio, M.; Croatto, G.; Dorigatti, G.; Turrini, U. Nested Buildings: An Innovative Strategy for the Integrated Seismic and Energy Retrofit of Existing Masonry Buildings with CLT Panels. *Sustainability* **2021**, *13*, 1188. [[CrossRef](#)]
77. Tinsley, J.; Pavía, S. Thermal performance and fitness of glacial till for rammed earth construction. *J. Build. Eng.* **2019**, *24*, 100727. [[CrossRef](#)]
78. José, M.; Fiorito, F. Performance assessment of earth constructions under the Chilean energy rating system software. *Procedia Eng.* **2017**, *180*, 502–509. [[CrossRef](#)]
79. Palme, M.; Guerra, J.; Alfaro, S. Thermal Performance of Traditional and New Concept Houses in the Ancient Village of San Pedro De Atacama and Surroundings. *Sustainability* **2014**, *6*, 3321–3337. [[CrossRef](#)]
80. Bahramian, M.; Yetilmezsoy, K. Life cycle assessment of the building industry: An overview of two decades of research (1995–2018). *Energy Build.* **2020**, *219*, 109917. [[CrossRef](#)]
81. Santos, T.; Nunes, L.; Faria, P. Production of eco-efficient earth-based plasters: Influence of composition on physical performance and bio-susceptibility. *J. Clean. Prod.* **2018**, *167*, 55–67. [[CrossRef](#)]

82. WBCSD. *Decarbonizing Construction—Guidance for Investors and Developers to Reduce Embodied Carbon*; WBCSD: Geneva, Switzerland, 2021; p. 76.
83. Caldas, L.R.; Toledo Filho, R.D. Avaliação do Ciclo de Vida de materiais cimentícios utilizados no Brasil: Estudo para o bloco de concreto e diferentes argamassas. *LALCA Rev. Latino-Americana Avaliação Ciclo Vida* **2019**, *2*, 34–61. [[CrossRef](#)]
84. Qin, J.; Jiang, J.; Tao, Y.; Zhao, S.; Zeng, W.; Shi, Y.; Lu, T.; Guo, L.; Wang, S.; Zhang, X.; et al. Sunlight tracking and concentrating accelerated weathering test applied in weatherability evaluation and service life prediction of polymeric materials: A review American Society of Testing Materials. *Polym. Test.* **2021**, *93*, 106940. [[CrossRef](#)]
85. Silva, A.; Brito, J. De Service life of building envelopes: A critical literature review. *J. Build. Eng.* **2021**, *44*, 102646. [[CrossRef](#)]
86. Gursel, A.P.; Maryman, H.; Ostertag, C. A life-cycle approach to environmental, mechanical, and durability properties of “green” concrete mixes with rice husk ash. *J. Clean. Prod.* **2016**, *112*, 823–836. [[CrossRef](#)]
87. Petek Gursel, A.; Masanet, E.; Horvath, A.; Stadel, A. Life-cycle inventory analysis of concrete production: A critical review. *Cem. Concr. Compos.* **2014**, *51*, 38–48. [[CrossRef](#)]
88. Gettu, R.; Patel, A.; Rathi, V.; Prakasan, S.; Basavaraj, A.S.; Palaniappan, S.; Maity, S. Influence of supplementary cementitious materials on the sustainability parameters of cements and concretes in the Indian context. *Mater. Struct. Constr.* **2019**, *52*, 10. [[CrossRef](#)]
89. Paiva, R.L.M.; Martins, A.P.S.; Caldas, L.R.; Reales, O.A.M.; Filho, R.D.T. Earth-based mortars: Mix design, mechanical characterization and environmental performance assessment. In Proceedings of the 4th International Conference on Bio-Based Building Materials (ICBBM 2021), Barcelona, Spain, 16–18 June 2021; pp. 362–367.
90. Caldas, L.R.; Toledo Filho, R.D. Avaliação ambiental do sistema construtivo de alvenaria de blocos de solo-cimento considerando diferentes especificações de projeto. *Gestão Tecnol. Proj.* **2021**, *16*, 149–172. [[CrossRef](#)]
91. Arrigoni, A.; Beckett, C.T.S.; Ciancio, D.; Pelosato, R.; Dotelli, G.; Grillet, A.C. Rammed Earth incorporating Recycled Concrete Aggregate: A sustainable, resistant and breathable construction solution. *Resour. Conserv. Recycl.* **2018**, *137*, 11–20. [[CrossRef](#)]
92. Pacheco-Torgal, F.; Jalali, S. Earth construction: Lessons from the past for future eco-efficient construction. *Constr. Build. Mater.* **2012**, *29*, 512–519. [[CrossRef](#)]